Imaging Pituitary Vasopressin 1B Receptor in Humans with the PET Radiotracer ^{11}C-TASP699

Mika Naganawa[1], Nabeel B. Nabulsi[1], David Matuskey[1], Shannan Henry[1], Jim Ropchan[1], Shu-Fei Lin[1], Hong Gao[1], Richard Pracitto[1], David Labaree[1], Ming-Rong Zhang[2], Tetsuya Suhara[2], Izumi Nishino[3], Helene Sabia[4], Satoshi Ozaki[4], Yiyun Huang[1], and Richard E. Carson[1]

[1]*Yale PET Center, Department of Radiology and Biomedical Imaging, Yale University, New Haven, Connecticut;* [2]*National Institutes for Quantum and Radiological Science and Technology, Chiba, Japan;* [3]*Taisho Pharmaceutical Co., Ltd., Tokyo, Japan; and* [4]*Taisho Pharmaceutical R&D Inc., Morristown, New Jersey*

Arginine vasopressin is a hormone that is synthesized mainly in the hypothalamus and stored in the posterior pituitary. Receptors for vasopressin are categorized into at least 3 subtypes (V_{1A}, V_{1B}, and V_2). Among these subtypes, the V_{1B} receptor (V_{1B}R), highly expressed in the pituitary, is a primary regulator of hypothalamic-pituitary-adrenal axis activity and thus a potential target for treatment of neuropsychiatric disorders such as depression and anxiety. *N-tert*-butyl-2-[2-(6-methoxypyridine-2-yl)-6-[3-(morpholin-4-yl)propoxy]-4-oxopyrido[2,3-d]pyrimidin-3(4*H*)-yl]acetamide (TASP699) is a novel PET radiotracer with high affinity and selectivity for V_{1B}R. The purpose of this study was to characterize the pharmacokinetic and binding profiles of ^{11}C-TASP699 in humans and determine its utility in an occupancy study of a novel V_{1B}R antagonist, TS-121. **Methods:** Six healthy subjects were scanned twice with ^{11}C-TASP699 to determine the most appropriate kinetic model for analysis of imaging data and test–retest reproducibility of outcome measures. Nine healthy subjects were scanned before and after administration of TS-121 (active component: THY1773) to assess V_{1B}R occupancy. Metabolite-corrected arterial input functions were obtained. Pituitary time–activity curves were analyzed with 1- and 2-tissue-compartment (1TC and 2TC, respectively) models and multilinear analysis 1 (MA1) to calculate distribution volume (V_T). Relative test–retest variability (TRV) and absolute TRV were calculated. Since no brain region could be used as a reference region, percentage change in V_T after TS-121 administration was computed to assess its receptor occupancy and correlate with plasma concentrations of the drug. **Results:** ^{11}C-TASP699 showed high uptake in the pituitary and no uptake in any brain region. The 2TC model provided better fits than the 1TC model. Because the MA1 V_T estimates were similar to the 2TC V_T estimates, MA1 was the model of choice. The TRV of V_T was good (TRV, $-2\% \pm 14\%$; absolute TRV, 11%). THY1773 reduced V_T in a dose-dependent fashion, with a half-maximal inhibitory concentration of 177 ± 52 ng/mL in plasma concentration. There were no adverse events resulting in discontinuation from the study. **Conclusion:** ^{11}C-TASP699 was shown to display appropriate kinetics in humans, with substantial specific binding and good reproducibility of V_T. Therefore, this tracer is suitable for measurement of V_{1B}R in the human pituitary and the V_{1B}R occupancy of TS-121, a novel V_{1B}R antagonist.

Key Words: PET; kinetic modeling; receptor imaging; pituitary; vasopressin V_{1B} receptor

J Nucl Med 2022; 63:609–614
DOI: 10.2967/jnumed.121.262430

Arginine vasopressin (AVP) is a key regulator of the hypothalamic-pituitary-adrenal axis. In response to stress exposure, AVP potentiates the effects of corticotropin-releasing factor on adrenocorticotropin release from pituitary corticotrophs (*1*). Among the 3 vasopressin receptor subtypes (V_{1A}, V_{1B}, and V_2), the V_{1B} receptor (V_{1B}R), which is expressed abundantly in the anterior pituitary (*2*), mediates the pituitary actions of AVP and regulates hypothalamic-pituitary-adrenal axis activity (*3*).

Several clinical studies have reported on the role of AVP in stress-related disorders. For example, AVP plasma levels were elevated in patients with major depressive disorder in comparison with healthy controls (*4*) and in depression with anxiety and slowed psychomotor activity (*5*). Cerebrospinal fluid AVP levels significantly decreased in patients who have major depressive disorder treated with the antidepressant fluoxetine, which is accompanied by a decrease in depression scores (*6*). In general, hyperactivity of the hypothalamic-pituitary-adrenal axis is a common finding in depression (*7,8*) and is thus a target of antidepressant treatment. These findings suggest that V_{1B}R antagonists may be indicated in the treatment of major depressive disorder via reducing hypothalamic-pituitary-adrenal axis activity (*9,10*).

Development of V_{1B}R imaging agents for PET will permit the in vivo characterization of this receptor subtype in humans, as well as accurate quantification of target engagement by drug candidates. To date, such development has been hampered by a lack of selective V_{1B}R ligands. A nonpeptide V_{1B}R antagonist, ^{11}C-SSR149415, was evaluated in nonhuman primates and shown to have minimal uptake in the brain and high uptake in the pituitary (*11*). However, human imaging of ^{11}C-SSR149415 has not been reported. More recently, a novel pyridopyrimidin-4-one analog, *N-tert*-butyl-2-[2-(6-methoxypyridine-2-yl)-6-[3-(morpholin-4-yl)propoxy]-4-oxopyrido[2,3-d]pyrimidin-3(4*H*)-yl]acetamide (TASP699), was identified as a V_{1B}R antagonist with high affinity and selectivity for V_{1B}R (V_{1B}, 0.16 nM; 87 other off-target molecules including V_{1A}, V_2, and oxytocin receptors, >1 μM) (*12*). The ^{11}C-labeled ligand ^{11}C-TASP699 was then developed as a PET radiotracer and shown to have high uptake in the monkey pituitary. Further, the pituitary uptake was dose-dependently inhibited by pretreatment with TASP0390325 (*12*), a selective V_{1B}R antagonist that has been well characterized in

Received Apr. 19, 2021; revision accepted Jul. 15, 2021.
For correspondence, contact Mika Naganawa (mika.naganawa@ yale.edu).
Published online Aug. 12, 2021.

pharmacologic studies (*13*), thus demonstrating the $V_{1B}R$ binding specificity of ^{11}C-TASP699.

The aim of this first-in-humans PET study was to evaluate the tracer ^{11}C-TASP699 for measurement of $V_{1B}R$ availability, in order to assess the reproducibility of binding parameters. An open-label, single-dose study was also done to determine the target occupancy of a novel $V_{1B}R$ antagonist TS-121 (*14*) in the pituitary and to evaluate the relationship between plasma exposure of THY1773 (active component of TS-121) and receptor occupancy.

MATERIALS AND METHODS

Human Subjects

This was a 2-part study: test–retest and receptor occupancy. Fifteen healthy men were enrolled (test–retest: $n = 6$, 37–50 y old, body weight of 88 ± 11 kg; occupancy: $n = 9$, 32–52 y old, body weight of 80 ± 10 kg). Individuals were excluded if they had a diagnosis of a current or lifetime psychiatric disorder, a diagnosis of a current or past serious medical or neurologic illness, metal in the body that would result in an MRI contraindication, or a history of substance abuse or dependence. PET imaging experiments were conducted under a protocol approved by the Yale University School of Medicine Human Investigation Committee and the Yale–New Haven Hospital Radiation Safety Committee and were in accordance with U.S. federal guidelines and regulations for the protection of human research subjects (title 45, part 46, of the *Code of Federal Regulations*). Written informed consent was obtained from all subjects. MR images were acquired on all subjects to verify the absence of brain structural abnormalities. MRI was performed on a 3-T whole-body scanner (Trio; Siemens Medical Systems). The dimensions and pixel size of MR images were 256 × 256 × 176 voxels and 0.98 × 0.98 × 1.0 mm^3, respectively.

Safety assessments included monitoring of adverse events and serious adverse events, routine hematology, biochemistry and urinalysis testing, physical and neurologic examinations, vital signs and electrocardiograms, concomitant medications, and extent of exposure (^{11}C-TASP699 exposure in terms of radioactivity [MBq] per kilogram of body weight and total radioactivity, and, for part 2, extent of exposure to TS-121 in terms of milligrams of drug per kilogram of body weight at admission).

Radiotracer Synthesis

^{11}C-TASP699 (Fig. 1) was radiolabeled with ^{11}C-CH_3I as reported previously (*12*). The PET drug was purified by high-performance liquid chromatography (Luna C18(2) [Phenomenex], 10 μm, 10 × 250 mm, 25% acetonitrile/75% 0.1 M ammonium formate with 0.5% acetic acid, pH 4.2, at 5 mL/min and 254 nm), isolated by solid-phase extraction, and formulated in 10 mL of saline containing 1 mL of ethanol. The detailed radiosynthesis procedure is described in the supplemental materials (available at http://jnm.snmjournals.org).

PET Imaging Experiments

Six subjects underwent two 2-h ^{11}C-TASP699 PET scans on a single day to measure the reproducibility of the binding parameters in part 1 of the study. The start of the 2 scans were separated by 5.3 ± 0.7 h. In part 2 of the study, 9 subjects completed three 90-min PET scans (baseline, postdose 1, and postdose 2) to assess $V_{1B}R$ occupancy in the pituitary after a single oral administration of TS-121. The TS-121 dose was adaptively determined (3 mg, $n = 1$; 10 mg, $n = 3$; 30 mg, $n = 2$; 50 mg, $n = 3$). Postdose 1 scans were acquired 2.3 h after the dose of TS-121, and postdose 2 scans were acquired 1 or 2 d after the dose of TS-121 (3 mg, 2 d; 10 mg, 1 d; 30 mg, 2 d; 50 mg, 1 d [$n = 2$] and 2 d [$n = 1$]). The concentrations of THY1773 in plasma at pre-, mid-, and postscanning were determined by liquid chromatography and tandem mass spectrometry at CMIC, Inc., on behalf of Taisho Pharmaceutical Co., Ltd. The measured concentrations were averaged and used as the mean plasma exposure for each postdose scan.

All PET scans were conducted on a High Resolution Research Tomograph (Siemens Medical Solutions), which acquires 207 slices (1.2-mm slice separation) with a reconstructed image resolution of about 3 mm in full width at half maximum. After a 6-min transmission scan for attenuation correction, PET scans were acquired in list mode after intravenous administration of ^{11}C-TASP699 over 1 min by an automatic pump (Harvard PHD 22/2000; Harvard Apparatus). Dynamic scan data were reconstructed in 33 (test–retest) or 27 (occupancy) frames (6 × 0.5 min, 3 × 1 min, 2 × 2 min, 22 or 16 × 5 min) with corrections for attenuation, normalization, scatter, randoms, and dead time using the MOLAR algorithm (*15*). Event-by-event motion correction (*16*) was included in the reconstruction on the basis of measurements with the Polaris Vicra sensor (NDI Systems) with reflectors mounted on a swim cap worn by the subject.

In 4 scans, the Vicra motion-tracking signal was unstable or lost because of slippage of the cap. In these cases, head motion was estimated by registration of the emission images reconstructed without attenuation or scatter corrections, and then dynamic PET images were reconstructed using the estimated motion. For 4 other scans, slight residual motion was visible; each image frame was therefore aligned to the early average image from 0 to 10 min after injection.

Input Function Measurement

Arterial input functions were generated for all scans. Discrete blood samples were manually drawn every 10 s from 10 to 90 s, every 15 s from 90 s to 3 min, and then at 3.5, 5, 6.5, 8, 12, 15, 20, 25, 30, 45, 60, 75, 90, 105, and 120 min. In addition to samples for the whole-blood and plasma radioactivity curves, arterial blood samples were drawn to determine the unmetabolized fraction of tracer at 3, 8, 15, 30, 60, and 90 min for test–retest scans and at 5, 15, 30, 60, and 90 min for occupancy scans. Radiometabolite analysis was performed using the column-switching high-performance liquid chromatography method (*17*). Briefly, plasma was separated from the whole blood by centrifugation. Up to 5 mL of filtered plasma samples treated with urea (8 M) were injected into the automatic column-switching system equipped with a capture column (19 × 4.6 mm) packed with Phenomenex SPE Strata-X sorbent and a Luna C18(2) analytic column (5 μm, 4.6 × 250 mm) eluting with 1% acetonitrile in water at a flow rate of 2 mL/min for the first 4 min and then with a mobile phase of 31% acetonitrile and 69% 0.1 M ammonium formate (v/v) at 1.85 mL/min. The unmetabolized parent fraction was determined as the ratio of the sum of radioactivity in fractions containing the parent compound (retention time of ~10.5 min) to the total radioactivity collected and was fitted with an inverted γ-function.

For 1 baseline scan, reliable metabolite data were not available; the parent fraction curve at the postdose 2 study was therefore used to calculate a metabolite-corrected input function. For 1 postdose 2 scan, arterial blood samples were not available; the input function from the

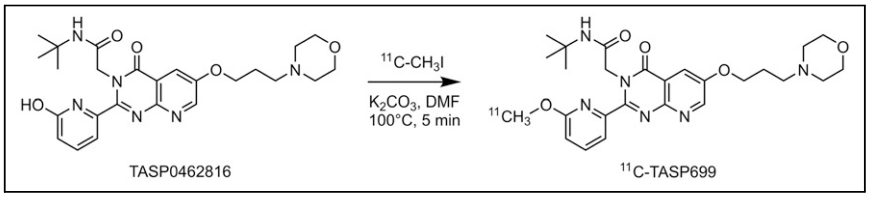

FIGURE 1. Synthesis of ^{11}C-TASP699. DMF = dimethylformamide.

baseline scan was therefore scaled using the ratio of the injected doses between the 2 scans.

An ultrafiltration-based method was used to measure the unbound portion (free fraction) of ^{11}C-TASP699 in plasma (*18*).

Quantitative Analysis

Analysis was performed directly on the PET images. A pituitary region of interest (ROI) was determined as the 400 voxels (730 mm^3) with the highest values on the SUV image (test–retest scans, 10–120 min; occupancy scans, 10–90 min), and a pituitary time–activity curve was generated. The ROI was chosen to be larger than the pituitary size to reduce variability across frames. The regional distribution volume (V_T) was computed using 1-tissue- and 2-tissue-compartment (1TC and 2TC, respectively) models and the multilinear analysis 1 (MA1) method. The effect of inclusion of a blood volume term was also assessed. The *F* test was used to compare model fits. Data points were weighted on the basis of noise-equivalent counts in each frame. Percentage SE was estimated from the theoretic parameter covariance matrix.

The mean and SD of the test–retest variability (TRV) was calculated as follows:

$$\mathrm{TRV} = 100 \times \frac{V_T^{\mathrm{retest}} - V_T^{\mathrm{test}}}{\left(V_T^{\mathrm{retest}} + V_T^{\mathrm{test}}\right)/2}. \qquad \text{Eq. 1}$$

Mean TRV is an index of trend in V_T values between test and retest scans, and the SD of TRV is an index of the variability of the percentage difference between the 2 measurements. The absolute value of TRV, which combines these 2 effects into a single value, was also computed.

The time stability of pituitary V_T values was assessed by comparing V_T values from scans shortened from 110 to 50 min with V_T values from 120-min scans in the test–retest dataset. Two criteria were used to determine a minimum scan duration (*19*): the average of the ratio was between 0.95 and 1.05, and the interindividual SD of the ratio was less than 0.1.

For the occupancy study, the fractional difference, that is, apparent receptor occupancy (*aRO*), between baseline and postdose V_T values was computed using the following formula, which also shows the physiologic interpretation of *aRO*:

$$aRO = 1 - \frac{V_T^{\text{post-dose}}}{V_T^{\text{baseline}}} = 1 - \frac{V_{ND}(1 + BP_{ND}(1 - RO))}{V_{ND}(1 + BP_{ND})} = RO\frac{BP_{ND}}{1 + BP_{ND}}. \qquad \text{Eq. 2}$$

V_{ND} is the nondisplaceable volume of distribution, BP_{ND} is the pituitary binding potential with respect to the nondisplaceable pool, and *RO* is the true receptor occupancy. Since *aRO* is proportional to *RO,* the half-maximal inhibitory concentration (IC_{50}) of THY1773 can be estimated with the following formula using the plasma concentration and *aRO*:

$$aRO = aRO_{max}\frac{C}{IC_{50} + C}. \qquad \text{Eq. 3}$$

where aRO_{max} is the maximum possible value of *aRO* [$BP_{ND}/(1 + BP_{ND})$] and *C* is the THY1773 plasma concentration during each scan.

All modeling was performed with in-house programs using IDL 8.0 (ITT Visual Information Solutions).

RESULTS

Radiochemistry

^{11}C-TASP699 was prepared in 24% ± 6% radiochemical yield based on trapped ^{11}C-CH_3I (range, 7.3%–44.1% for n = 41, decay-corrected to the end of bombardment). At the end of synthesis, the radiochemical and chemical purities were 97% ± 2% and 99% ± 7%, respectively, and the molar activity was 1,017.1 ± 465.0 GBq/μmol (173.5–1910 GBq/μmol). The average synthesis time was 46 ± 2 min.

Injection Parameters and Plasma Analysis

Table 1 lists the injected radioactivity dose, molar activity at time of injection, injected mass, and plasma free fractions. There were no significant differences between test and retest scans or between baseline and postdose scans. The administered activity of ^{11}C-TASP699 was 569 ± 169 MBq (range, 301–756 MBq) for the test–retest study and 533 ± 118 MBq (range, 312–707 MBq) for the occupancy study. There were no adverse or clinically detectable pharmacologic effects by the administered radiotracer in any subject. No significant changes in vital signs or the results of laboratory studies were observed.

Figure 2 shows the mean (±SD) of parent fractions and metabolite-corrected plasma curves. In part 1, the mean parent fractions at 30 min were 71% ± 7% for the test scans (n = 6) and 69% ± 6% for the retest scans (n = 6), and in part 2, the mean parent fractions at 30 min were 70% ± 3% for the baseline scans, 69% ± 3% for postdose scan 1, and 69% ± 6% for postdose scan 2. The free fraction of ^{11}C-TASP699 in plasma was 48% ± 6% (n = 12) for the test–retest scans, 50% ± 7% (n = 9) for the baseline scans, 51% ± 5% (n = 9) for postdose scan 1, and 52% ± 6% (n = 9) for postdose scan 2. The free fraction displayed no difference between test and retest scans or between baseline and postdose scans.

Modeling Results

High uptake of ^{11}C-TASP699 was reliably seen in the pituitary, with no substantial uptake in brain regions such as the choroid plexus and pineal gland (Fig. 3B). Pituitary regional time–activity curves for ^{11}C-TASP699 (Fig. 4) showed peak uptake at approximately 10–30 min after injection followed by gradual clearance. Typical examples of fits are shown in Figure 4A. The pituitary time–activity curve was fitted well with the 2TC and MA1 models, and the *F* test showed that 2TC fitting was better than the 1TC model ($P < 0.05$ in 11 of 12 fits). However, the 2TC model provided unstable V_T estimation (relative SE > 10%) and physiologically implausible microparameters (relative SE of K_1 and k_2 > 100%). The mean pituitary K_1 from 1TC was 0.10 ± 0.02 mL/cm^3/min. 1TC V_T was somewhat underestimated compared with the reliable 2TC values but correlated well with 2TC V_T estimates ($V_{T,1TC} = 0.91 \times V_{T,2TC} + 0.11$, $R^2 = 0.99$). MA1 V_T estimates were similar to those from 2TC with a good correlation ($V_{T,MA1,t^* = 10\ \mathrm{min}} = 0.97 \times V_{T,2TC} + 0.21$, $R^2 = 1.00$). Since the MA1 method provided reliable V_T estimates (relative SE < 10%) similar to those from 2TC, the MA1 V_T values were used in the following analysis.

MA1 V_T values showed large intersubject variability, ranging from 3.6 to 9.7 mL/cm^3 (n = 19; test, retest, and baseline scans), and approximately 15 mL/cm^3 for 1 subject, which may have been caused in part by the ROI definition. Note, however, that the TRV and absolute TRV were reasonably good (TRV, −2% ± 14%; absolute TRV, 11%; intraclass correlation coefficient, 0.94) (Fig. 5A), indicating good reliability of the measurements from repeated scans. The V_T estimates for all models did not change with the inclusion of 2 additional parameters: a blood volume term and the time delay between the blood sampling site and pituitary. The percentage differences were 3% ± 3% for 1TC, 4% ± 3% for 2TC, and 0% ± 2% for MA1. Many 2TC V_T values were unstable with the addition of

TABLE 1
PET Scan Parameters

Parameter	Test–retest (n = 6)		Occupancy (n = 9)		
	Test	Retest	Baseline	Postdose 1	Postdose 2
Injected dose (MBq)	618 ± 134	519 ± 196	528 ± 126	540 ± 132	532 ± 109
Injected mass (μg)	0.90 ± 0.57	0.75 ± 0.59	1.16 ± 1.13	1.19 ± 1.19	0.93 ± 0.48
Plasma free fraction	47% ± 5%	50% ± 7%	50% ± 7%	51% ± 5%	52% ± 6%

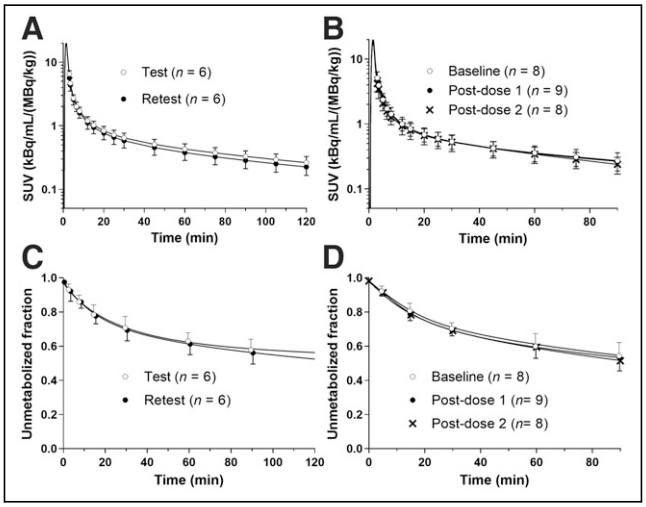

FIGURE 2. Mean ± SD of total plasma activity and parent fraction in plasma in test and retest scans (A and C) and in baseline, postdose 1, and postdose 2 scans (B and D).

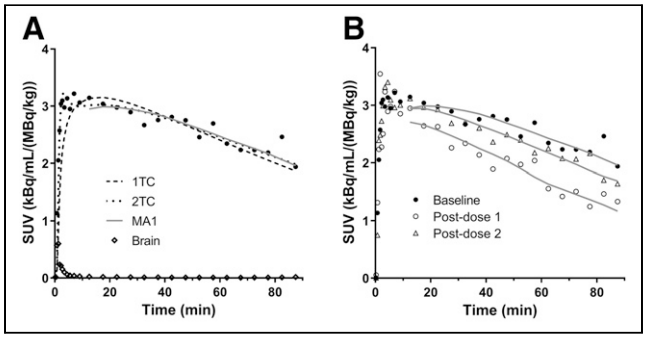

FIGURE 4. (A) Representative pituitary time–activity curve in baseline scan with 1TC (dashed), 2TC (dotted), and MA1 (t^* = 10 min, solid) fits with brain time–activity curve. (B) Pituitary time–activity curves in baseline, postdose 1, and postdose 2 conditions with MA1 fits.

delay and blood volume parameters (8/20 fits), and these values were excluded from this comparison. Pituitary blood volume was estimated to be about 20%. The minimum scan time for stable MA1 V_T estimates was 90 min. The percentage difference in V_T with respect to 120-min estimate was −6% ± 13%, −2% ± 16%, 1% ± 14%, 1% ± 9%, 0% ± 6%, and 0% ± 3% for the 60-, 70-, 80-, 90-, 100-, and 110-min scans.

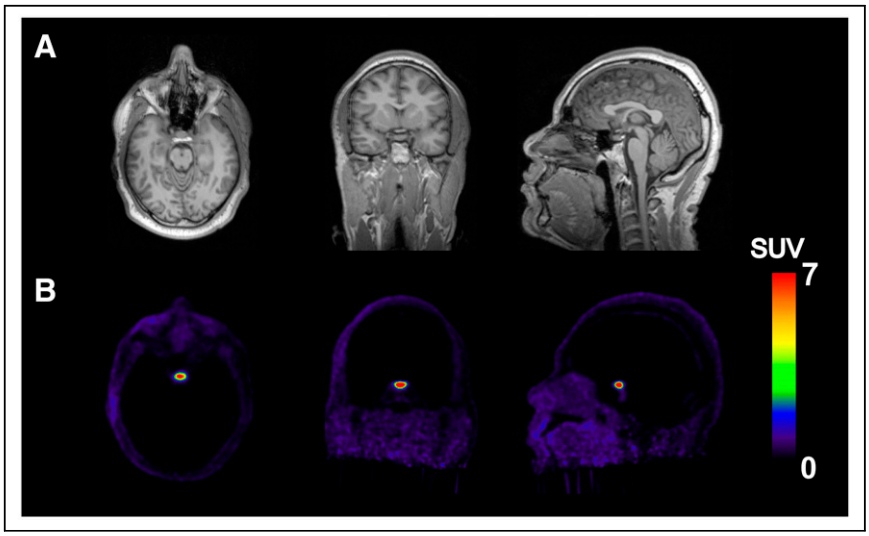

FIGURE 3. Typical MR (A) and coregistered PET images summed from 30 to 120 min after injection of ^{11}C-TASP699. Coregistration (rigid transform) was applied using extracranial uptake (blue or purple area).

Occupancy Results

Figure 4B shows a set of pituitary time–activity curves from the baseline and postdose scans after a 10-mg dose of TS-121. A moderate blocking effect was observed in the pituitary region. Figure 5B summarizes the percentage reductions in V_T in the pituitary using MA1, whereas Figure 6 shows a plot of the percentage change in V_T with THY1773 concentration in the plasma. The THY1773 plasma concentration over time is shown in Supplemental Figure 1. Using Equation 3, the IC_{50} (mean ± SE) was estimated at 177 ± 52 ng/mL, with an aRO_{max} of 62% ± 7%. Using the estimated aRO_{max} and Equation 2, the pituitary binding potential (BP_{ND}), representing the equilibrium ratio of specific to nondisplaceable binding, was calculated to be 1.6. Using the estimated aRO_{max}, percentage change in V_T was converted to RO, shown as the y-axis on the right of Figure 6.

In fitting PET-measured occupancy values, it is typically assumed that the plasma drug levels are an accurate reflection of the drug levels in the tissue. This assumption may not be met at early times, depending on how rapidly the drug enters the tissue (*20*). We thus assessed whether the occupancy values at all times were consistent by using the F test to compare regression

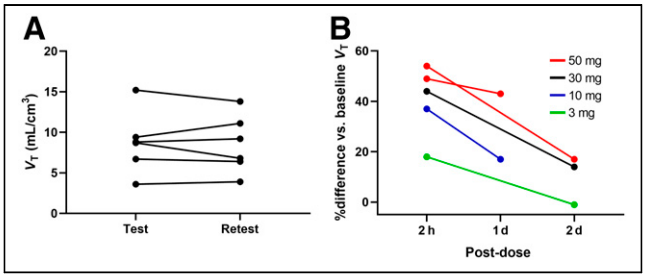

FIGURE 5. (A) Pituitary V_T values in test and retest conditions. Each symbol corresponds to a subject. (B) Mean percentage difference in V_T in comparison with baseline V_T values (*aRO*) at 2 h, 1 d, and 2 d after administration of TS-121.

curve fits of Equation 3. The null hypothesis was that 1 set of model parameters was appropriate for all postdose scans. The alternative hypothesis was that a different curve was needed for the postdose scan 1 data versus the postdose scan 2 data, because of potential hysteresis. The null hypothesis was not rejected ($P = 0.29$). Therefore, hysteresis was not considered in the estimation. However, the ability to detect hysteresis may be limited since the data points for postdose 1 and postdose 2 scans were centered on different concentrations of the curve.

Safety

Overall, no safety issues were identified that would prevent further development and testing of either the investigational radiotracer ^{11}C-TASP699 or the investigational drug TS-121.

No adverse events or serious adverse events resulting in discontinuation from the study (pain or burning at or arterial line or injection site was the most common adverse event, occurring in 3 subjects). No apparent safety trends in clinical laboratory results, vital sign measurements, electrocardiogram results, or physical and neurologic examinations were observed.

DISCUSSION

This first-in-humans PET study was conducted to assess the ability of a novel V_{1B}R antagonist PET radiotracer, ^{11}C-TASP699, to image V_{1B}R in the human pituitary. Modeling methods were evaluated on the basis of time–activity curves and metabolite-corrected input functions. The volume of distribution was determined and used to estimate receptor occupancy by the V_{1B}R antagonist, TS-121. A clear relationship between plasma concentration of the drug and receptor occupancy was found.

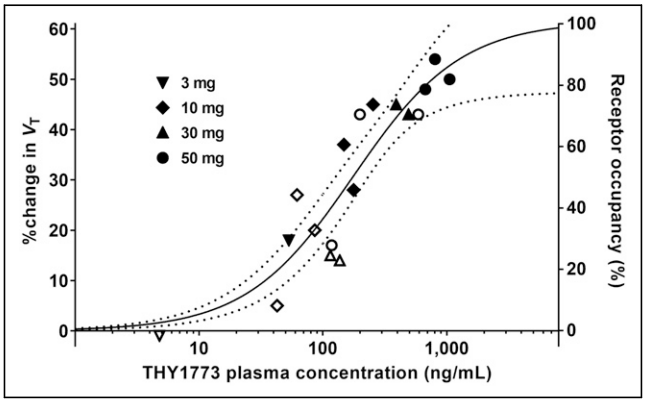

FIGURE 6. Relationship between THY1773 plasma concentrations and percentage change in V_T (left *y*-axis) and receptor occupancy (right *y*-axis). Estimated IC_{50} and aRO_{max} are 177 ± 52 ng/mL and 62% ± 7%, respectively. Solid symbols and open symbols denote postdose 1 and postdose 2, respectively.

Modeling analysis assumes that only parent compound enters tissue and binds to the receptor. However, radiolabeled metabolites are likely to access the pituitary, since it has no blood–brain barrier. If the magnitude of the metabolite effect is large, it may bias the results. This does not seem to have been the case in the current study, since, first, V_T did not show a continuous increase with scan time, as would be expected from tissue uptake of metabolites, and second, the metabolite fraction in plasma was moderate. In addition, since the fraction of metabolites was similar in the baseline and postdose scans, even if radiolabeled metabolites were present and were incorrectly increasing the estimated V_T values, the IC_{50} estimates would likely not be affected although the aRO_{max} could be biased.

Large intersubject variability was seen in V_T (4–10 mL/cm^3), although the test–retest reproducibility was good (absolute TRV, 11%). We evaluated whether there was a relationship between V_T estimates at baseline scans and subject age, weight, body mass index, scan starting time, and injected mass, but we found no significant effects. V_T might be affected by the pituitary volume itself, since it varies by age, sex, season, and subject conditions (*21–23*). However, we were not able to accurately define pituitary volumes from MR images since separation of the pituitary from neighboring tissues was challenging in many cases. Thus, we used a standard ROI size. Mean pituitary volume in healthy men is 500 ± 79 mm^3 (*22*), and a larger ROI (730 mm^3) was used to ensure that all uptake was included. To further consider this factor, the effect of ROI size on V_T values was evaluated. As expected, V_T values increased with smaller ROI sizes because of a reduced partial-volume effect. A near-identical TRV was found for ROIs above 500 mm^3 (TRV, −3% ± 15% with 550 mm^3 and −2% ± 13% with 910 mm^3). Thus, the large intersubject variability in V_{1B}R could have some biologic meaning. There have been several studies using immunohistochemistry, reverse-transcription polymerase chain reaction, and in situ hybridization histochemistry to investigate V_{1B}R distribution in rodents. However, to the best of our knowledge, there are no quantitative postmortem studies in humans or nonhuman primates.

For the 2 subjects for whom plasma or metabolite data were not available from one scan, the data from another scan were used to generate the input function. We evaluated the effect of using these data from other scans in the subjects for whom all data were available. Percentage differences in V_T were 1% ± 8% (plasma) and 0% ± 4% (metabolites).

Using ^{11}C-TASP699, we evaluated the V_{1B}R occupancy of TS-121, a drug candidate targeted for major depressive disorder. On the basis of animal model experience with THY1773, attenuated hyperactivity of the hypothalamic-pituitary-adrenal axis and antidepressantlike effects were found with more than 50% pituitary V_{1B}R occupancy. This study showed that 10–50 mg of TS-121 achieved more than 50% occupancy at 2 h after a single oral administration in healthy men (Fig. 6). A phase 2 clinical trial using TS-121 (*14*) in patients with major depressive disorder showed reductions in the Montgomery-Asberg Depression Rating Scale score for subjects who had a daily oral TS-121 dose of 10 or 50 mg at week 6, though these reductions did not achieve statistical significance. If the plasma concentration was similar in both groups (patients with major depressive disorder with daily dosing, and our healthy subjects with a single administration), the dose of 10–50 mg should have been sufficient. However, plasma concentration may differ between

patients and healthy subjects, as was seen in a glycine transporter-1 inhibitor study (*24*) in which the IC_{50} was similar between healthy controls and schizophrenic patients but the ID_{50} values were significantly different.

CONCLUSION

The novel V_{1B}R antagonist tracer ^{11}C-TASP699 showed high uptake in the pituitary but did not enter the brain. Its tracer kinetics could be modeled using MA1 to quantify V_T values. V_T values were variable between subjects but showed good test–retest reproducibility. ^{11}C-TASP699 was successfully used in an occupancy study, which showed a consistent relationship between THY1773 (active component of TS-121) plasma concentration and V_{1B}R occupancy. Single oral doses of TS-121 (3, 10, 30, and 50 mg) were found to be safe and well tolerated.

DISCLOSURE

This study was funded by Taisho Pharmaceutical R&D Inc. Izumi Nishino is a full-time employee of Taisho Pharmaceutical Co., Ltd. Satoshi Ozaki and Helene Sabia are a full-time employees of Taisho Pharmaceutical R&D Inc. Ming-Rong Zhang and Tetsuya Suhara hold a patent for ^{11}C-TASP699 (Japan patent JP2015-1206 44A). No other potential conflict of interest relevant to this article was reported.

ACKNOWLEDGMENTS

The clinical trial registration identifier of this study is NCT0244-8212. We appreciate the excellent technical assistance of the staff at the Yale University PET Center. We thank Dr. Shigeyuki Chaki for reviewing this manuscript.

KEY POINTS

QUESTION: Does ^{11}C-TASP699 show suitable kinetic properties to quantify pituitary V_{1B}R in humans?

PERTINENT FINDINGS: The novel V_{1B}R antagonist tracer ^{11}C-TASP699 showed a good test–retest reproducibility. The tracer showed high uptake in the pituitary but did not enter the brain. The occupancy of TS-121 increased in a dose-dependent fashion (IC_{50} was 177 ng/mL as THY1773).

IMPLICATIONS FOR PATIENT CARE: ^{11}C-TASP699 provides excellent measurements of V_{1B}R binding in the human pituitary.

REFERENCES

1. Aguilera G, Rabadan-Diehl C. Vasopressinergic regulation of the hypothalamic-pituitary-adrenal axis: implications for stress adaptation. *Regul Pept.* 2000;96:23–29.
2. Serradeil-Le Gal C, Raufaste D, Derick S, et al. Biological characterization of rodent and human vasopressin V1b receptors using SSR-149415, a nonpeptide V1b receptor ligand. *Am J Physiol Regul Integr Comp Physiol.* 2007;293:R938–R949.
3. Tanoue A, Ito S, Honda K, et al. The vasopressin V1b receptor critically regulates hypothalamic-pituitary-adrenal axis activity under both stress and resting conditions. *J Clin Invest.* 2004;113:302–309.
4. van Londen L, Goekoop JG, van Kempen GM, et al. Plasma levels of arginine vasopressin elevated in patients with major depression. *Neuropsychopharmacology.* 1997;17:284–292.
5. de Winter RF, van Hemert AM, DeRijk RH, et al. Anxious-retarded depression: relation with plasma vasopressin and cortisol. *Neuropsychopharmacology.* 2003; 28:140–147.
6. De Bellis MD, Gold PW, Geracioti TD Jr, Listwak SJ, Kling MA. Association of fluoxetine treatment with reductions in CSF concentrations of corticotropin-releasing hormone and arginine vasopressin in patients with major depression. *Am J Psychiatry.* 1993;150:656–657.
7. Scott LV, Dinan TG. Vasopressin and the regulation of hypothalamic-pituitary-adrenal axis function: implications for the pathophysiology of depression. *Life Sci.* 1998;62:1985–1998.
8. Inder WJ, Donald RA, Prickett TC, et al. Arginine vasopressin is associated with hypercortisolemia and suicide attempts in depression. *Biol Psychiatry.* 1997;42:744–747.
9. Griebel G, Stemmelin J, Gal CS, Soubrie P. Non-peptide vasopressin V1b receptor antagonists as potential drugs for the treatment of stress-related disorders. *Curr Pharm Des.* 2005;11:1549–1559.
10. Roper J, O'Carroll AM, Young W III, Lolait S. The vasopressin Avpr1b receptor: molecular and pharmacological studies. *Stress.* 2011;14:98–115.
11. Schönberger M, Leggett C, Kim SW, Hooker JM. Synthesis of [^{11}C]SSR149415 and preliminary imaging studies using positron emission tomography. *Bioorg Med Chem Lett.* 2010;20:3103–3106.
12. Koga K, Nagai Y, Hanyu M, et al. High-contrast PET imaging of vasopressin V1B receptors with a novel radioligand, ^{11}C-TASP699. *J Nucl Med.* 2017;58:1652–1658.
13. Iijima M, Yoshimizu T, Shimazaki T, et al. Antidepressant and anxiolytic profiles of newly synthesized arginine vasopressin V1B receptor antagonists: TASP0233278 and TASP0390325. *Br J Pharmacol.* 2014;171:3511–3525.
14. Kamiya M, Sabia HD, Marella J, et al. Efficacy and safety of TS-121, a novel vasopressin V1B receptor antagonist, as adjunctive treatment for patients with major depressive disorder: a randomized, double-blind, placebo-controlled study. *J Psychiatr Res.* 2020;128:43–51.
15. Carson RE, Barker WC, Liow JS, Johnson CA. Design of a motion-compensation OSEM list-mode algorithm for resolution-recovery reconstruction for the HRRT. *IEEE 2003 Nucl Sci Symp Conf Rec.* 2003;5:3281–3285.
16. Jin X, Chan C, Mulnix T, et al. List-mode reconstruction for the Biograph mCT with physics modeling and event-by-event motion correction. *Phys Med Biol.* 2013;58:5567–5591.
17. Hilton J, Yokoi F, Dannals RF, Ravert HT, Szabo Z, Wong DF. Column-switching HPLC for the analysis of plasma in PET imaging studies. *Nucl Med Biol.* 2000;27: 627–630.
18. Li S, Cai Z, Zheng MQ, et al. Novel ^{18}F-labeled κ-opioid receptor antagonist as PET radiotracer: synthesis and in vivo evaluation of ^{18}F-LY2459989 in nonhuman primates. *J Nucl Med.* 2018;59:140–146.
19. Frankle WG, Huang Y, Hwang DR, et al. Comparative evaluation of serotonin transporter radioligands ^{11}C-DASB and ^{11}C-McN 5652 in healthy humans. *J Nucl Med.* 2004;45:682–694.
20. Naganawa M, Gallezot JD, Rossano S, Carson RE. Quantitative PET imaging in drug development: estimation of target occupancy. *Bull Math Biol.* 2019;81:3508–3541.
21. Lurie SN, Doraiswamy PM, Husain MM, et al. In vivo assessment of pituitary gland volume with magnetic resonance imaging: the effect of age. *J Clin Endocrinol Metab.* 1990;71:505–508.
22. Schwartz PJ, Loe JA, Bash CN, et al. Seasonality and pituitary volume. *Psychiatry Res.* 1997;74:151–157.
23. Büschlen J, Berger GE, Borgwardt SJ, et al. Pituitary volume increase during emerging psychosis. *Schizophr Res.* 2011;125:41–48.
24. D'Souza DC, Carson RE, Driesen N, et al. Dose-related target occupancy and effects on circuitry, behavior, and neuroplasticity of the glycine transporter-1 inhibitor PF-03463275 in healthy and schizophrenia subjects. *Biol Psychiatry.* 2018;84: 413–421.